ACS APPLIED MATERIALS & INTERFACES

Letter

www.acsami.org

Determination of Isoelectric Points and the Role of pH for Common Quartz Crystal Microbalance Sensors

Michael F. Cuddy,* Aimee R. Poda, and Lauren N. Brantley

Environmental Laboratory, U.S. Army Corps of Engineer Research and Development Center, 3909 Halls Ferry Road, Vicksburg, Mississippi 39180, United States

ABSTRACT: Isoelectric points (IEPs) were determined by the method of contact angle titration for five common quartz crystal microbalance (QCM) sensors. The isoelectric points range from mildly basic in the case of Al_2O_3 sensors (IEP = 8.7) to moderately acidic for Au (5.2) and SiO_2 (3.9), to acidic for Ag (3.2) and Ti (2.9). In general, the values reported here are indicative of inherent surface oxides. A demonstration of the effect of the surface isoelectric point on the packing efficiency of thin mucin films is provided for gold and silica QCM sensors. It is determined that mucin layers on both substrates achieve a maximum and equal layer density of ~3500 kg/m^3 at the corresponding IEP of either QCM sensor. This implies that mucin film packing is dependent upon short-range electrostatic interactions at the sensor surface.

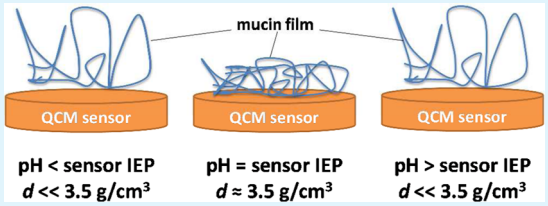

KEYWORDS: *isoelectric point, IEP, quartz crystal microbalance, QCM, sensor, mucin*

INTRODUCTION

The isoelectric point (IEP) of a material dictates many key aspects, including its electrical properties and application potential for catalysis[1,2] and adhesion.[3] Although IEPs for many metals/metal oxides can be found in the literature,[4,5] such values are often representative of pristine surfaces analyzed under ideal conditions. Moreover, explicit measurements of coating IEPs for quartz crystal resonators used in QCM investigations have not, to the best of our knowledge, been carried out. To elucidate fundamental surface properties of quartz crystal microbalance (QCM) sensors, we have measured IEPs for five different sensors under practical application conditions. These conditions include manufacturer-prescribed cleaning methods such as ultraviolet light/ozone exposure which may induce surface oxide growth. Recent work by Tabor and co-workers demonstrated that a single monolayer oxide on a gold surface is sufficient to shift the surface potential inversion point (isoelectric point) by ~2 pH units. This suggests that condition-specific measurements of IEP are crucial for subsequent materials applications and experimental design.

Here, we employed the method of contact angle (CA) titration as a function of pH to determine IEPs. This method has previously been employed to measure IEPs for both metal[6] and metal oxide[7−9] surfaces. Assuming uniform surface composition with some overall net charge, the CA of a droplet on the surface follows a second-order polynomial relationship with respect to pH. A best-fit regression line to the experimental data yields the IEP, or the pH value corresponding to the maximum of the polynomial. A straightforward demonstration of the effect of IEP on film deposition is demonstrated for porcine gastric mucin binding to Au and SiO_2.

EXPERIMENTAL SECTION

Ten solutions of varying pH, from 0.90 to 13.31, were prepared by diluting either concentrated HCl (reagent grade, Sigma-Aldrich) or NaOH (99.4%, Calbiochem) in 18 MΩ cm deionized water. Liquid-surface contact angles at each pH were measured for alumina, gold, silica, silver, and titanium QCM sensors (all QSense, see Table 1). Each sensor was cleaned and UV/O_3-treated in accordance with recommended protocol[10−14] prior to each CA measurement. Contact angles of sessile liquid droplets of ~2 μL were analyzed within 2 s of dispense using a Kernco goniometer. Measurements were repeated in triplicate. CA values were plotted as a function of the corresponding pH and fit with a quadratic function using the mathematics tool MATlab. A method for error propagation, based on the work of the Fisher group,[8,9] was developed to handle data processing. Briefly, this routine fits all possible

Table 1. Isoelectric Points and Maximum Water Contact Angle Values Determined from Second-Order Polynomial Fits to Titration Data for Five QSense QCM Sensors

sensor	isoelectric point pH (error)	water contact angle at IEP (deg)
Al_2O_3 (QSX309)	8.7 (0.4)	56
Au (QSX301)	5.2 (0.2)	59
SiO_2 (QSX303)	3.9 (0.5)	8
Ag (QSX322)	3.2 (1.6)	52
Ti (QSX310)	2.9 (0.1)	42

Received: March 12, 2013
Accepted: April 23, 2013
Published: April 23, 2013

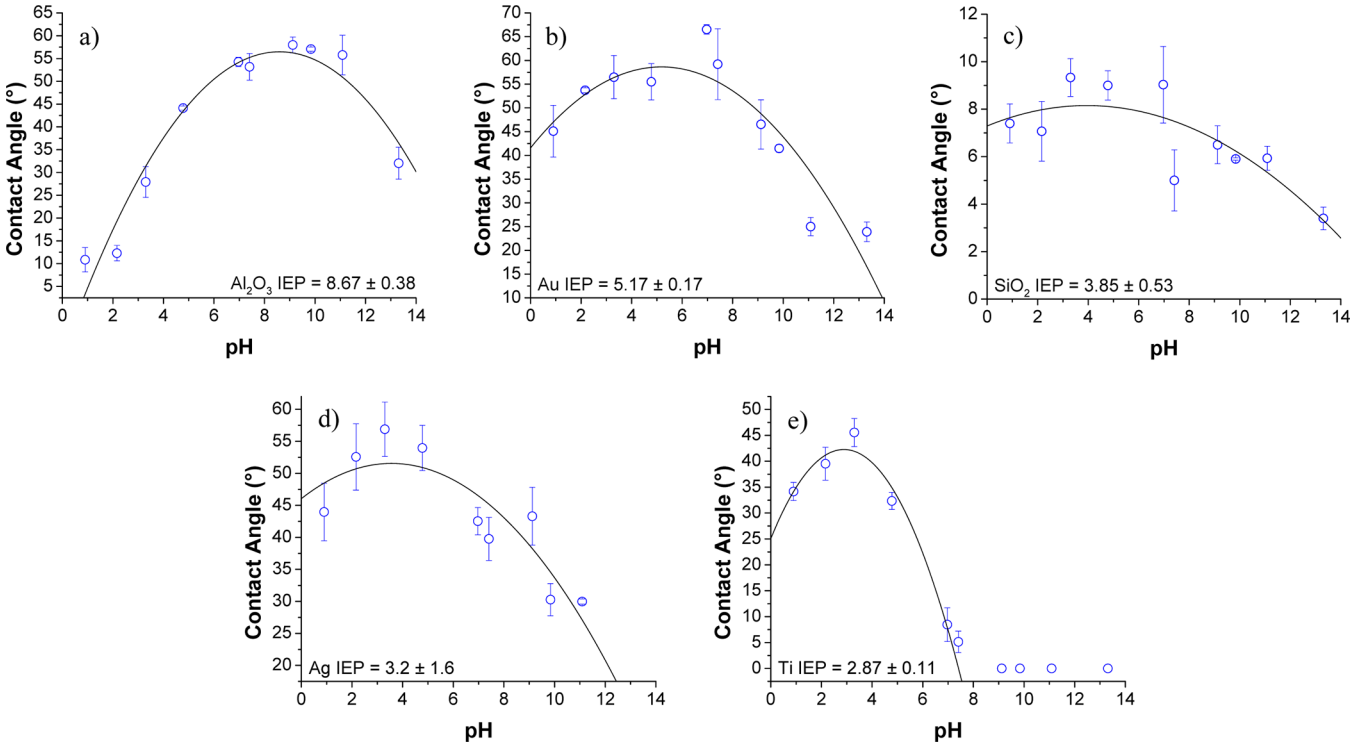

Figure 1. Contact angles plotted as a function of corresponding droplet pH and fit with a second-order polynomial. The pH of the fit maximum determines the isoelectric point for each sensor. Here, the IEP values are (a) 8.7 for Al_2O_3, (b) 5.2 for Au, (c) 3.9 for SiO_2, (d) 3.2 for Ag, and (e) 2.9 for Ti.

scenarios wherein the standard deviation of the mean of three replicates is taken into account. Simultaneously, the routine iteratively differentiates individual fits and compares root values to propagate total error of the fit to the entire data set. This ensures that data outliers are adequately addressed in the reported IEP value. For CAs indicative of instantaneous wetting (as in the case for Ti with pH > 8), these values were omitted from the fitting routine.

Porcine stomach mucin (Sigma-Aldrich CAS# 84082−64−4) was prepared at 25 mg/L in pH 3.0, 4.1, 5.0, and 6.6 stock solutions. Thirty millimolar NaCl solutions were prepared at the same pH values. A recent report suggests that quartz crystal microbalance investigations of porcine mucin binding can be confounded by changes in sensor surface roughness induced by repeated use.[15] Therefore, clean, fresh sensors were utilized for each of these investigations. QCM measurements were performed by first priming the sensor with NaCl at a given pH, followed by mucin at the same pH, with a final rinse in NaCl. All flow rates were maintained at 150 μL/min using an Ismatec four-channel peristaltic pump. A QSense E4 quartz crystal microbalance with dissipation monitoring (QCM-D) was used to collect the measurements.

RESULTS AND DISCUSSION

Figure 1 shows experimental data along with the fits used to determine IEPs for five QCM sensors. A tabulated list of IEP values, including propagated error, and the maximum contact angle at the best-fit maximum for each sensor are summarized in Table 1. It is of interest to compare the IEP values obtained in this work to those found in the literature. A multitude of data exist in the literature regarding IEPs for alumina surfaces that shows that the IEP is dependent upon crystal structure. For α-Al_2O_3, reported IEPs range from 8.4 to 9.2, whereas the range for γ-Al_2O_3 is 7.4−8.6.[16] Amorphous alumina exhibits an IEP of ~9.2.[16] Our data (IEP = 8.7, Figure 1a) suggest that the Al_2O_3 QCM sensors are most strongly associated with the α-Al_2O_3 (close-packed) structure. Gold is reported in various sources to have IEP = 4.5,[17] 5,[18] or 4−6.[19] A caveat to these values, as illustrated by Tabor and co-workers,[19] is that surface oxidation of the gold results in a shift toward more basic IEPs. These values generally agree well with our measured value of 5.2 (Figure 1b), and so suggest minimal-to-moderate surface oxidation of the QCM sensor. Literature values for IEP(SiO_2) include 3.5 for fused silica glass,[20] 3.9 for native oxide on a Si wafer,[9] and 5.6 for a thick SiO_2 film grown by plasma-enhanced chemical vapor deposition.[9] Our analysis indicates that the SiO_2 sensors (IEP = 3.9, Figure 1c) exhibit surface charge characteristics very similar to Si wafers with a native oxide layer. Perusal of the literature yields few IEP values for silver metal. Chau and Porter reported an IEP of 10.4 for an evaporated silver film as determined by contact angle titration.[6] The method employed in their investigation used only neutral and basic liquids, and the maximum contact angle achieved on the silver films was ~35°, in contrast to the maximum we observe of 52° at pH 3.2 (Figure 1d). This dichotomy may be indicative of the amphoteric behavior of the native oxide at the surface. Pinzari and co-workers[21] examined the wettability of titanium sheets, concluding that pure Ti exhibits a basic IEP whereas the oxidized form is more acidic. In addition, Hanly, et al.[22] determined that sputtered TiO_2 films have an isoelectric point of 4.4. Our reported value, 2.9, is significantly more acidic. Notably, our data show near-instantaneous wetting of the Ti sensor for pH >8, Figure 1e, that resulted in unquantifiable CAs for basic droplets. This case suggests that the IEP of the Ti sensor, in particular, is strongly influenced by surface oxide.

dx.doi.org/10.1021/am400909g | ACS Appl. Mater. Interfaces 2013, 5, 3514−3518

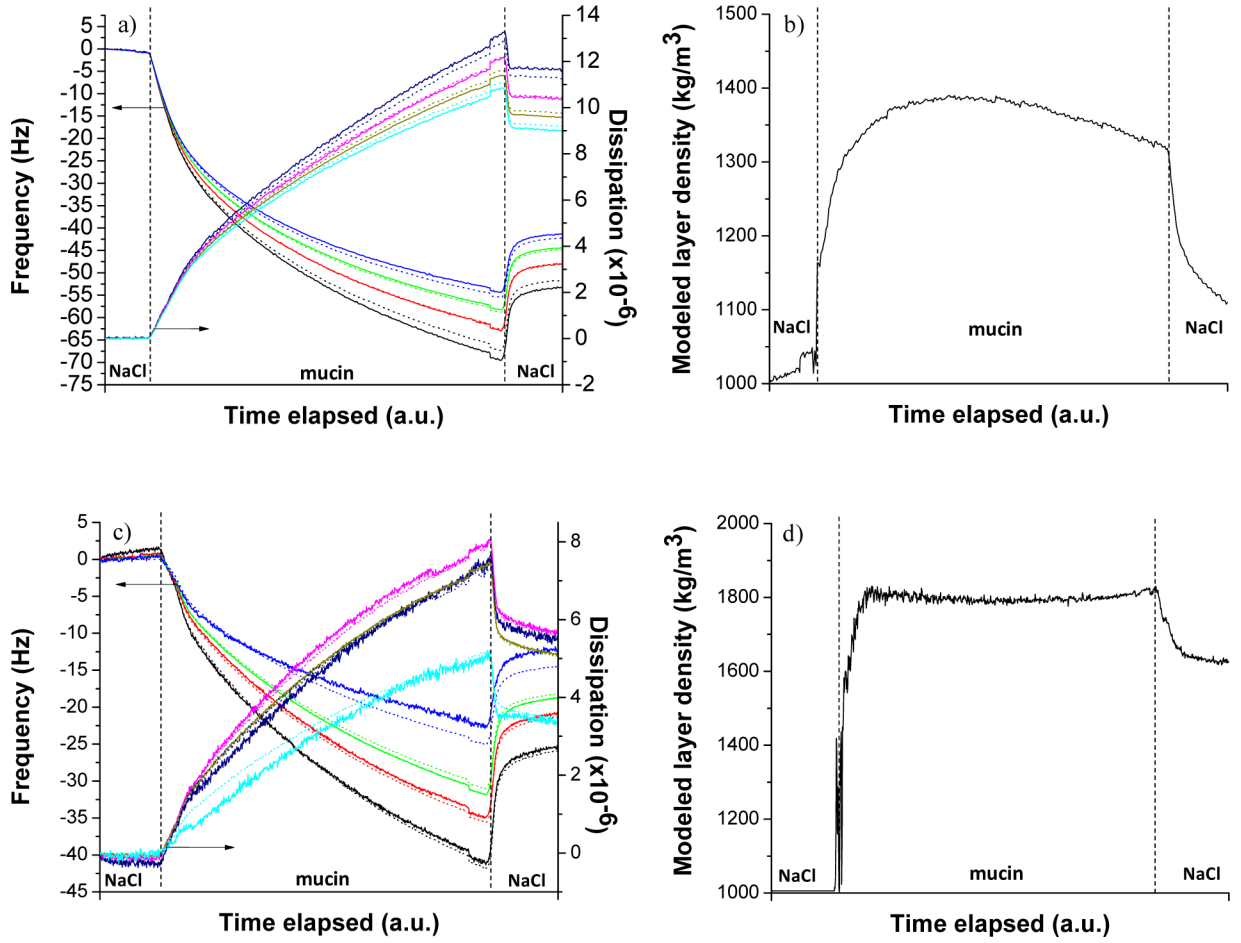

Figure 2. Frequency (left ordinate) and dissipation (right ordinate) QCM responses are plotted as solid lines for the n = 5, 7, 9, and 11 overtones of (a) Au and (c) SiO_2 sensors. Both sensors were exposed first to NaCl solution, followed by porcine mucin, with a final rinse in NaCl (all solutions were prepared at pH 3.0). Viscoelastic model fits to the data are plotted as corresponding dotted lines. The fits yielded mucin layer densities plotted at a function of elapsed experiment time for (b) Au and (d) SiO_2, respectively. An average density of 1344 kg/m^3 was determined for mucin deposited on the gold sensor under these conditions, whereas the average density for mucin deposited on SiO_2 was 1796 kg/m^3.

To illustrate the effect of pH on IEP-dependent processes, the binding of gastric mucin to gold and silica sensors was investigated by QCM. Au and SiO_2 were selected for their facilitation of efficacious mucin deposition. Mucins are glycoproteins with ideal electrostatic properties suited to investigation of protein−surface binding dynamics. Generally, mucins consist of charged amino acid residues with a mildly acidic amino acid backbone and significantly more acidic side chains.[23] As such, the overall charge of the glycoprotein is dictated by pH; the isoelectric point of mucin lies between 2 and 3.[24] Investigations of mucin deposition by QCM with dissipation monitoring facilitated determination of film properties for the viscoelastic films. Here, frequency (f) and dissipation (D) are coupled according to eqs 1 and 2,

$$\Delta f = \left(\frac{n}{\pi}\right)^{1/2} f_s^{3/2} \frac{1}{\rho_q v_q} \sqrt{\rho_l \eta_l} \quad (1)$$

$$\Delta D = 2\left(\frac{f_s}{n\pi}\right)^{1/2} \frac{1}{\rho_q v_q} \sqrt{\rho_l \eta_l} \quad (2)$$

where η is the dynamic viscosity of the material of interest, ρ is the film density, v_q is the speed of sound in quartz (3340 m/s), n is the overtone number, and f_s is the fundamental resonance frequency of the sensor (nominally 4.95 Hz). The n = 5−11 overtones were monitored for modeling purposes, and these data were fit with a Voigt viscoelastic model to achieve minimum residual χ^2 and to determine layer shear, density, and thickness as a function of experiment duration. The layer viscosity values used in the models were estimated from the work of Bhaskar et al.[25]

Representative frequency and dissipation data for pH 3.0 plotted as a function of elapsed experiment time are shown in Figure 2a and c for Au and SiO_2 sensors, respectively. Generally, a decrease in frequency is directly proportional to mass gain at the sensor surface, whereas an increase in dissipation is indicative of softer (less rigid) films. Thus, a cursory comparison of the mucin films suggests that although more material is deposited on Au compared to SiO_2 sensors, the material on Au is less rigid.

These plots also illustrate the viscoelastic fits to the data as dotted lines. Figure 2b and d show the corresponding layer density as determined from the model. Density values for the mucin regions were averaged to yield mucin densities of 1344 kg/m^3 on Au sensors and 1796 kg/m^3 on SiO_2 at pH 3.0. Similar measurements were carried out for three additional systems of increasing pH. Average mucin film densities are provided as a function of pH in Figure 3. The maximum mucin layer density for Au sensors, ∼3500 kg/m^3, was found at pH

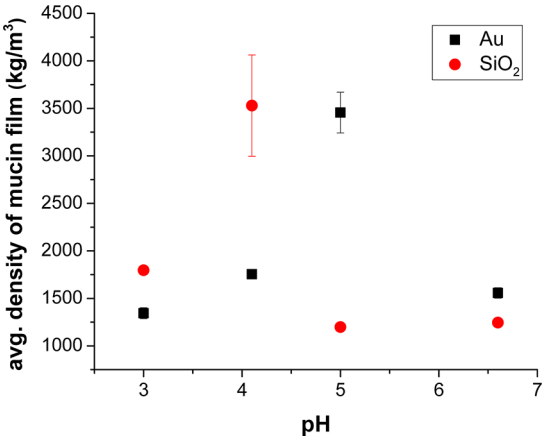

Figure 3. Average densities determined from viscoelastic models to QCM-D data for gold (black squares) and SiO_2 (red circles) sensors are plotted as a function of the corresponding pH of the NaCl/mucin solutions to which the sensors were exposed. The density of mucin films on Au sensors reaches a maximum at pH 5, whereas the maximum density for a mucin film on SiO_2 is near pH 4. Error bars represent the standard deviation of the mean of at least three trials. The IEP values were 5.2 and 3.9 for Au and SiO_2, respectively.

5.0, very near the experimentally determined IEP of the Au sensor (5.2 ± 0.2). Similarly, the maximum mucin density on SiO_2, also ~3500 kg/m^3, was found at pH = 4.1, within error of the sensor IEP of 3.9 ± 0.5. The large variability observed in the density of mucin on SiO_2 and Au near the respective IEPs of the sensors is likely a result of inconsistencies associated with the modeled fit to the experimental QCM data. As mentioned above, the layer viscosity values for the mucin films were based on Bhaskar et al.'s work and kept fixed at a given pH. Because the viscosity and density are codependent (eqs 1 and 2), large changes in the density are expected to coincide with similarly significant changes in viscosity. These parameters cannot be simultaneously modeled, so the ramifications of fixed values for viscosities in the viscoelastic model manifests in greater potential for variability in the modeled fits to the layer density. This variability is especially apparent in the layer density determined for mucin on SiO_2 at pH 4.1.

Notably, despite the observation that a larger mass of material was deposited on Au sensors than on SiO_2 sensors at any set of conditions (data not shown), the mucin film densities on each sensor achieved essentially the same maximum value at the corresponding IEP of the sensor. At pH < 4, porcine mucin has an anisotropic, extended conformation which induces gelation at concentrations exceeding 10 mg/mL.[26] At pH >4, mucin readily assumes a random coil conformation[27] that facilitates hydrogen bonding and van der Waals and hydrophobic interactions.[28] This ostensibly exposes negatively charged subunits around a central hydrophobic core. Indeed, a previous investigation[29] on the role of surface charge for mucin interactions showed that positively charged polystyrene microspheres effectually permeate gastrointestinal mucin layers, contrary to negatively charged spheres. This phenomenon was ascribed to the effect of the negatively charged oligosaccharides. Our data show that substrate electronic effects are critical for efficient packing of thin mucin layers. It is inferred that short-range interactions between the sensor surface and bound layer impede efficient mucin packing via electrostatic repulsion when the surface itself possesses some net charge. At a pH near the sensor IEP, these repulsive forces are mitigated, thereby promoting the coalescence of a denser mucin film. The influence of substrate isoelectric point on the preferential packing of mucin films demonstrates that the surface IEP is a key aspect of consideration for materials investigations and applications.

CONCLUSIONS

The isoelectric points of five commonly used QCM sensors have been determined by the method of contact angle titration. We have determined that the IEPs are largely indicative of surface oxides begot by ordinary sensor cleaning, as the values generally agree with the reported literature values for corresponding metal oxides. The effect of IEP on the binding of porcine gastric mucin was investigated by QCM and the results demonstrated that mucin films deposit most densely when the pH of the mucin solution matches the sensor isoelectric point. Thus, electrostatic interactions should be considered for QCM applications wherein adsorption behavior is likely to be influenced by the sensor IEP.

AUTHOR INFORMATION

Corresponding Author

*E-mail: Michael.Cuddy@usace.army.mil, +1 601.634.4820.

Notes

The authors declare no competing financial interest.

ACKNOWLEDGMENTS

The use of trade, product, or firm names in this report is for descriptive purposes only and does not imply endorsement by the U.S. Government. The tests described and the resulting data presented herein, unless otherwise noted, were obtained from research conducted under the Environmental Quality Technology Program of the United States Army Corps of Engineers by the USAERDC. Permission was granted by the Chief of Engineers to publish this information. The findings of this report are not to be construed as an official Department of the Army position unless so designated by other authorized documents. The authors also thank Frances Hill and Andrea Scott of the USACE for their editorial comments.

REFERENCES

(1) Santhanam, N.; Conforti, T. A.; Spieker, W.; Regalbuto, J. R. *Catal. Today* **1994**, *21* (1), 141−156.
(2) Benesi, H. A.; Winquist, B. H. C.; Eley, D.D.; , H. P.; Paul, B. W. Surface Acidity of Solid Catalysts. In *Advances in Catalysis*; Academic Press: \New York, 1979; Vol. *27*, pp 97−182.
(3) Rijnaarts, H. H. M.; Norde, W.; Lyklema, J.; Zehnder, A. J. B. *Colloids Surf., B* **1995**, *4* (4), 191−197.
(4) *Encyclopedia of Surface and Colloid Science*; Somasundaran, P., Ed.; CRC Press: Boca Raton, FL, 2006.
(5) Kung, H. H. *Transition Metal Oxides: Surface Chemistry and Catalysis*; Elsevier: New York, 1991.
(6) Chau, L.-K.; Porter, M. D. *J. Colloid Interface Sci.* **1991**, *145* (1), 283−286.
(7) McCafferty, E.; Wightman, J. P. *J. Colloid Interface Sci.* **1997**, *194* (2), 344−355.
(8) Trevino, K. J.; Shearer, J. C.; McCurdy, P. R.; Pease-Dodson, S. E.; Okegbe, C. C.; Fisher, E. R. *Surf. Interface Anal.* **2011**, *43* (9), 1257−1270.
(9) Trevino, K. J.; Shearer, J. C.; Tompkins, B. D.; Fisher, E. R. *Plasma Process. Polym.* **2011**, *8* (10), 951−964.
(10) Kern, W.; Puotinen, D. A. *RCA Rev.* **1970**, *31*, 187−206.
(11) Harewood, K.; Wolff Iii, J. S. *Anal. Biochem.* **1973**, *55* (2), 573−581.

(12) Penfold, J.; Staples, E.; Tucker, I.; Thomas, R. K. *Langmuir* **2002**, *18* (15), 5755−5760.
(13) Olofsson, A.-C.; Hermansson, M.; Elwing, H. *Appl. Environ. Microbiol.* **2005**, *71* (5), 2705−2712.
(14) Kwon, K. D.; Green, H.; Bjoorn, P.; Kubicki, J. D. *Environ. Sci. Technol.* **2006**, *40* (24), 7739−7744.
(15) Znamenskaya, Y.; Sotres, J.; Gavryushov, S.; Engblom, J.; Arnebrant, T.; Kocherbitov, V. *J. Phys. Chem. B* **2013**, *117* (8), 2554−2563.
(16) Parks, G. A. *Chem. Rev.* **1965**, *65* (2), 177−198.
(17) Giesbers, M.; Kleijn, J. M.; Cohen Stuart, M. A. *J. Colloid Interface Sci.* **2002**, *248* (1), 88−95.
(18) Barten, D.; Kleijn, J. M.; Duval, J.; Lyklema, J.; Cohen Stuart, M. A. *Langmuir* **2003**, *19* (4), 1133−1139.
(19) Tabor, R. F.; Morfa, A. J.; Grieser, F.; Chan, D. Y. C.; Dagastine, R. R. *Langmuir* **2011**, *27* (10), 6026−6030.
(20) Sabia, R.; Ukrainczyk, L. *J. Non-Cryst. Solids* **2000**, *277* (1), 1−9.
(21) Pinzari, F.; Ascarelli, P.; Cappelli, E.; Giorgi, R.; Turtu, S. *Appl. Surf. Sci.* **2000**, *156* (1−4), 1−8.
(22) Hanly, G.; Fornasiero, D.; Ralston, J.; Sedev, R. *J. Phys. Chem. C* **2011**, *115* (30), 14914−14921.
(23) Lee, S.; Muller, M.; Rezwan, K.; Spencer, N. D. *Langmuir* **2005**, *21* (18), 8344−8353.
(24) Bansil, R.; Turner, B. S. *Curr. Opin. Colloid Interface Sci.* **2006**, *11*, 164−170.
(25) Bhaskar, K. R.; Gong, D. H.; Bansil, R.; Pajevic, S.; Hamilton, J. A.; Turner, B. S.; LaMont, J. T. *Am. J. Physiol. Gastrointest. Liver Physiol.* **1991**, *261* (5), G827−G832.
(26) Celli, J.; Gregor, B.; Turner, B.; Afdhal, N. H.; Bansil, R.; Erramilli, S. *Biomacromolecules* **2005**, *6* (3), 1329−1333.
(27) Cao, X.; Bansil, R.; Bhaskar, K. R.; Turner, B. S.; LaMont, J. T.; Niu, N.; Afdhal, N. H. *Biophys. J.* **1999**, *76* (3), 1250−1258.
(28) Bansil, R.; Stanley, E.; LaMont, J. T. *Annu. Rev. Physiol.* **1995**, *57*, 635−657.
(29) Norris, D. A.; Sinko, P. J. *J. Appl. Polym. Sci.* **1997**, *63* (11), 1481−1492.